ISSN 0023-1584, Kinetics and Catalysis, 2017, Vol. 58, No. 2, pp. 122–132. © Pleiades Publishing, Ltd., 2017.
Original Russian Text © N.V. Ulitin, K.A. Tereshchenko, A.K. Frizen, A.O. Burakova, S.V. Kolesov, D.A. Shiyan, N.E. Temnikova, 2017, published in Kinetika i Kataliz, 2017, Vol. 58, No. 2, pp. 133–144.

Kinetic Scheme and Rate Constants for Methyl Methacrylate Synthesis Occurring via the Radical–Coordination Mechanism

N. V. Ulitin[a, *], K. A. Tereshchenko[a], A. K. Frizen[b], A. O. Burakova[a], S. V. Kolesov[b], D. A. Shiyan[a], and N. E. Temnikova[b]

[a] *Kazan National Research Technological University, Kazan, 420015 Tatarstan, Russia*

[b] *Ufa Institute of Chemistry, Russian Academy of Sciences, Ufa, 450054 Bashkortostan, Russia*

**e-mail: n.v.ulitin@mail.ru*

Received March 17, 2016

Abstract—Two kinetic schemes of the bulk radical–coordination polymerization of methyl methacrylate initiated by the benzoyl peroxide–ferrocene system are considered from the standpoint of formal kinetics. The most likely kinetic scheme is the one that includes the reactions characteristic of classical radical polymerization and, additionally, reactions of controlled radical polymerization proceeding via the Organometallic Mediated Radical Polymerization mechanism, a reaction generating a coordination active site, and a chain propagation reaction in the coordination sphere of the metal. The temperature dependences of the rate constants for the reactions of this kinetic scheme at temperatures typical of commercial poly(methyl methacrylate) production (313–353 K) have been determined by solving the inverse kinetic problem.

Keywords: radical–coordination polymerization, methyl methacrylate, macroinitiation, benzoyl peroxide, ferrocene, poly(methyl methacrylate), stereoregularity, molecular weight characteristics, inverse kinetic problem

DOI: 10.1134/S0023158417020136

Radical polymerization has a limited potential for producing polymers with preset molecular weight characteristics. This problem was solved by introducing, into the polymerizing mass, agents that can react reversibly with free radicals and hamper chain termination reactions—alkoxyamines, dithiocarbamates, transition metal halides, etc. [1–7]. This kind of polymerization is commonly called controlled radical polymerization and is also widely referred to as pseudo-living radical polymerization, living radical polymerization, and radical polymerization under living chain conditions [1, 5–7]. In the controlled radical polymerization, variation of the admixture concentration makes it possible to change the molecular weight characteristics of the polymer in fairly wide ranges [1–7]. Note that neither radical polymerization nor various methods of controlled radical polymerization provide mean to regulate the stereoregularity of the resulting polymer [5–7]. However, it was demonstrated in some works [8–13] that radical polymerization that takes place in the presence of metallocenes and has characteristic features of controlled radical polymerization yields polymers with an increased stereoregularity. Fairly extensive experimental data on the kinetics of radical polymerization in the presence of metallocenes and on the molecular weight characteristics and stereoregularity of the resulting polymer have been accumulated to date [8–18]. However, the observed regularities have not been considered from the standpoint of formal kinetics. There have been only hypotheses concerning the mechanisms of polymerization processes, which have been formulated on the basis of quantum chemical calculations [9, 19, 20]. According to these hypotheses, reactions involving the metallocene and components of the reaction mass can yield, in the reaction mass, coordination sites for polymerization and spin traps for chain carrier radicals. For this reason, in this study we considered the bulk radical–coordination polymerization of methyl methacrylate (MMA) initiated by benzoyl peroxide (BP) in the presence of ferrocene, found the most likely kinetic scheme for the process, and determined its rate constants as a function of temperature.

DETERMINATION OF THE KINETIC SCHEME OF THE PROCESS

The kinetic scheme of the process was determined using the following algorithm.

Initially, we left two possible kinetic schemes of the process. Both included the reactions involved in the bulk radical polymerization of MMA initiated by BP [21–25]:

initiator dissociation,

$$\mathrm{I} \xrightarrow{k_{\mathrm{diss}}} 2\mathrm{R}(0);$$

addition of the first monomer molecule to a free radical,

$$R(0) + M \xrightarrow{k_{prop1}} R(1);$$

chain propagation,

$$R(n) + M \xrightarrow{k_{prop1}} R(n+1), \quad n = 1,\ldots;$$

chain transfer to monomer,

$$R(n) + M \xrightarrow{k_{trans}} R(1) + P(n), \quad n = 1,\ldots;$$

recombination of radicals,

$$R(n) + R(z) \xrightarrow{k_{rec}} P(n+z), \quad n = 1,\ldots, \quad z = 1,\ldots;$$

disproportionation of radicals,

$$R(n) + R(z) \xrightarrow{k_{disp}} P(n) + P(z), \quad n = 1,\ldots, \quad z = 1,\ldots.$$

Here, I is the initiator; R(n) and P(n) are, respectively, the active radical and inactive polymer chain containing n MMA units; M is MMA; n and z are the numbers of MMA units in polymer chains; k stands for the rate constants of reactions. The structural formulas of I, R, P, and M are presented in Table 1.

Along with these reactions, reactions substantiated by quantum chemical calculations [9, 19] were included in the kinetic scheme:

formation of the BP–ferrocene complex [9, 19],

$$I + Mc \xrightarrow{k_{compl}} C;$$

chain initiation by the BP–ferrocene complex [9, 19],

$$C + M \xrightarrow{k_{in1}} R(1) + Ad_1(0);$$

chain initiation by the $[Cp_2Fe\cdots PhCOO]^{\bullet}$ adduct (Cp = cyclopentadienyl, Ph = phenyl) [19],

$$Ad_1(0) + M \xrightarrow{k_{in2}} R(1) + Mc;$$

formation of the metal-centered radical $CpFe^{\bullet}(CpR)$ [9],

$$Mc + R(n) \xrightarrow{k_{adduct1}} Ad_1(n), \quad n = 1,\ldots; \qquad (I)$$

recombination between the metal-centered radical and the chain carrier radical, yielding the CpFe(CpR)R adduct [9],

$$Ad_1(n) + R(z) \xrightarrow{k_{adduct2}} Ad(n,z), \quad n = 1,\ldots, \quad z = 1,\ldots;$$

formation of the monocyclopentadienyl adduct CpFe(MMA)(R) from the CpFe(CpR)R adduct [9],

$$Ad(n,z) + M \xrightarrow{k_{add1}} Ad_2(z) + P(n), \quad n = 1,\ldots, \quad z = 1,\ldots; \qquad (II)$$

formation of the coordination active site $CpFe(MMA)_2(R)$ via monomer coordination to the metal atom in the monocyclopentadienyl adduct CpFe(MMA)(R) [9],

$$Ad_2(z) + M \xrightarrow{k_{coord}} Ad_3(z), \quad z = 1,\ldots; \qquad (III)$$

coordinative chain propagation on the $CpFe(MMA)_2(R)$ active site due to the addition of a coordinated MMA molecule to the polymer chain in the sphere of the metal atom [9],

$$Ad_3(z) \xrightarrow{k_{prop2}} Ad_2(z+1), \quad z = 1,\ldots. \qquad (IV)$$

Here, C is the BP–ferrocene complex, Mc is ferrocene, $Ad_1(0)$ is the $[Cp_2Fe\cdots PhCOO]^{\bullet}$ adduct, $Ad_1(n)$ is the metal-centered radical $CpFe^{\bullet}(CpR)$ containing n MMA units in the chain, Ad(n, z) is the CpFe(CpR)R adduct containing n and z MMA units in the chains, $Ad_2(n)$ is the monocyclopentadienyl adduct CpFe(MMA)(R) containing n MMA units in the chain, and $Ad_3(n)$ is the coordination active site $CpFe(MMA)_2(R)$ containing n MMA units in the chain. The structural formulas of Ad, Ad_1, Ad_2, and Ad_3 are presented in Table 1.

Another kinetic scheme was composed as a competing hypothesis. This scheme is based on the assumption that the BP–ferrocene complex is unstable and decomposes spontaneously into an R(0) radical and an $Ad_1(0)$ adduct (without involving monomer molecules). In turn, the $Ad_1(0)$ adduct can decompose spontaneously into R(0) and metallocene. Guided by the same logic, we assumed that the compounds Ad(n, z), $Ad_2(z)$, and $Ad_3(z)$ can also decompose to produce radicals. Thus, the second kinetic scheme includes reactions typical of controlled radical polymerization occurring via the Organometallic Mediated Radical Polymerization (OMRP) mechanism, in which the metal complex serves as a spin trap for chain carrier radicals. In summary, the second kinetic scheme is comprised of the MMA radical polymerization reactions, the reaction yielding the metal-centered radical $CpFe^{\bullet}(CpR)$ (reaction (I)), the reactions that generate the coordination active site and are responsible for chain propagation in the coordination sphere of the metal (reactions (II)–(IV)), and the following reactions:

interaction between the initiator and ferrocene,

$$I + Mc \xrightarrow{k_{compl}} Ad_1(0) + R(0),$$

dissociation of the $[Cp_2Fe\cdots PhCOO]^{\bullet}$ adduct,

$$Ad_1(0) \xrightarrow{k_{diss1}} Mc + R(0),$$

reversible interaction between the chain carrier radical and the metal-centered radical $CpFe^{\bullet}(CpR)$ as a spin trap (in essence, this is an OMRP process; note that, on the basis of a quantum chemical simulation of the bulk radical–coordination polymerization of styrene in the presence of ferrocene, it was hypothesized [20] that the bond between the chain carrier radical and the metal atom in the CpFe(CpR)R adduct is too

Table 1. Designations and structural formulas of the compounds from the kinetic schemes

Designation	Structural formula	Designation	Structural formula
I	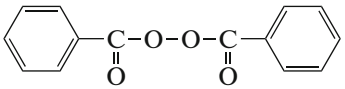	R(0)	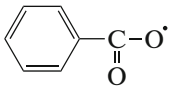
Mc		M	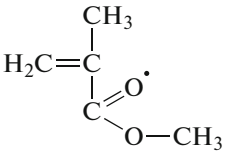
C	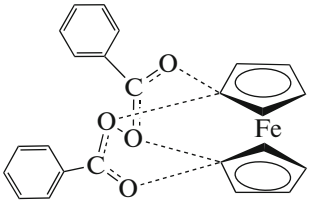	R(n)	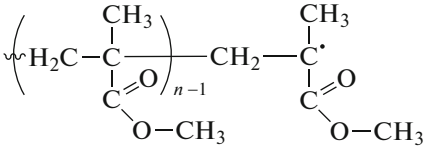
P(n)	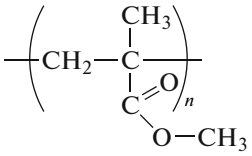	$Ad_1(n)$	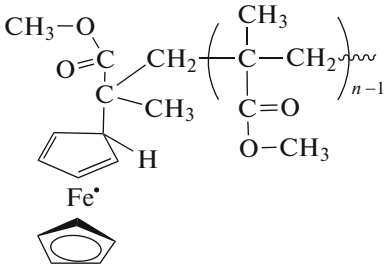
$Ad_1(0)$	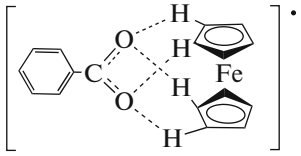	Ad(n, z)	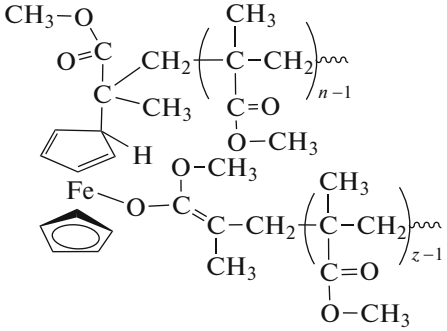
$Ad_2(z)$	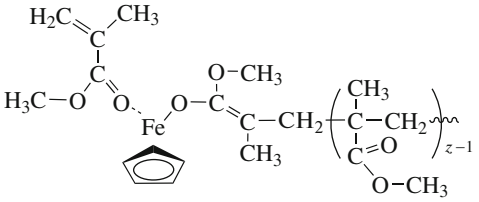	$Ad_3(z)$	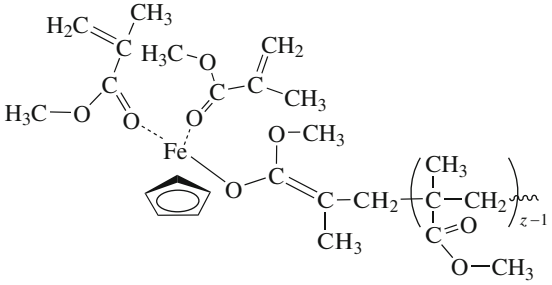
Mc'	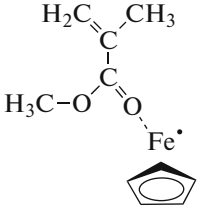	Mc"	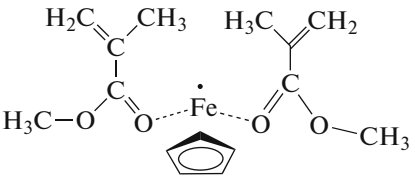

weak for the process to pass completely to the controlled regime owing to this reversible reaction),

$$R(z) + Ad_1(n) \underset{k_{diss\,2}}{\overset{k_{adduct\,2}}{\rightleftarrows}} Ad(n,z),$$
$$n = 1, \ldots, \quad z = 1,\ldots,$$

release of the chain carrier radical from the metal-centered adduct CpFe(MMA)(R) and the binding of the radical to the resulting species, CpFe$^{\bullet}$(MMA), i.e., OMRP equilibrium (the occurrence of this reversible reaction is assumed by analogy with the scheme of the bulk radical–coordination polymerization of styrene in the presence of ferrocene [20]),

$$Ad_2(z) \underset{k_{adduct\,3}}{\overset{k_{diss\,3}}{\rightleftarrows}} R(z) + Mc', \quad z = 1,\ldots,$$

release of the chain carrier radical from the coordination active site CpFe$(MMA)_2$(R) and the binding of the radical to the resulting species CpFe$^{\bullet}(MMA)_2$—this reaction can also be considered as OMRP,

$$Ad_3(z) \underset{k_{adduct\,4}}{\overset{k_{diss\,4}}{\rightleftarrows}} R(z) + Mc'', \quad z = 1,\ldots,$$

monomer coordination at vacant coordination sites of the iron atom in CpFe$^{\bullet}$(MMA)—the occurrence of this reaction was assumed by analogy with scheme of the bulk radical–coordination polymerization of styrene in the presence of ferrocene [20],

$$Mc' + M \xrightarrow{k_{add\,2}} Mc''.$$

Here, Mc' and Mc'' are ferrocene fragments in which one and two MMA molecules are coordinated to the iron atom, respectively. The structural formulas of Mc' and Mc'' are presented in Table 1.

Poly(methyl methacrylate) (PMMA), which results from the bulk radical–coordination polymerization process initiated by the BP–ferrocene system, can serve as a macroinitiator upon the addition of a new portion of the monomer—this is so-called postpolymerization, or the postprocess. The kinetic scheme of the postprocess consists of only reactions (III) and (IV). These reactions appear in both hypothetical kinetic schemes of the main process.

For either kinetic scheme, we wrote systems of kinetic equations according to the law of mass action. These systems were put into the following form by using the generating function method [26–28]:

$$\frac{d[I]}{dt} = f_1([I], [Mc], \ldots, k),$$
$$\frac{d[Mc]}{dt} = f_2([I], [Mc], \ldots, \mu_{qs}, k),$$
$$\frac{d[M]}{dt} = f_3([M],\ldots,\mu_{qs},\mu_{3pr}, k),$$
$$\ldots$$
$$\frac{d\mu_{qs}}{dt} = f_i([I], [Mc], [M],\ldots,\mu_{qs},\mu_{3pr}, k),$$
$$\ldots$$

where f_i designates the functions expressing the law of mass action, $\mu_{qs} = \sum_{n=1}^{\infty} n^s[X(n)]$ is the sth moment of the molecular weight distribution (where X = R, Ad_1, Ad_2, Ad_3, and P at the moment number q = 1, 2, 4, 5, and 6, respectively; $\mu_{3pr} = \sum_{n=1}^{\infty}\sum_{z=1}^{\infty} n^p z^r[Ad(n,z)]$ at $q = 3$ (p, r = 0, 1, 2)), and t is time.

The systems of equations in this form are mathematical models of the kinetics of the process considered. They provide means to calculate not only kinetic curves for the process but also the number-average molecular weight (M_n), weight-average molecular weight (M_w), and polydispersity index (PD) of PMMA:

$$M_n = m\frac{\mu_{11} + \mu_{21} + \mu_{310} + \mu_{301} + \mu_{41} + \mu_{51} + \mu_{61}}{\mu_{10} + \mu_{20} + \mu_{300} + \mu_{40} + \mu_{50} + \mu_{60}},$$
$$M_w = m\frac{\mu_{12} + \mu_{22} + \mu_{320} + 2\mu_{311} + \mu_{302} + \mu_{42} + \mu_{52} + \mu_{62}}{\mu_{11} + \mu_{21} + \mu_{310} + \mu_{301} + \mu_{41} + \mu_{51} + \mu_{61}},$$
$$PD = M_w/M_n,$$

where m is the molar mass of MMA.

In addition, these mathematical models make it possible to estimate the stereoregularity (γ) of PMMA from the concentration of MMA that has polymerized on each type of active site—radical site (rad) and coordination (stereoregulating, st):

$$\gamma = \frac{\gamma_{rad}[M_{rad}] + \gamma_{st}[M_{st}]}{[M]_0 - [M]},$$

where γ_{rad} = 56% is the stereoregularity of PMMA obtained on the radical active site [22], γ_{st} is the stereoregularity of PMMA obtained on the coordination active site, the subscript 0 at the monomer concentration [M] indicates that the MMA concentration at the initial point in time is considered, $[M_{rad}]$ and $[M_{st}]$ are the concentrations of MMA that has polymerized on the radical and coordination active sites, respectively:

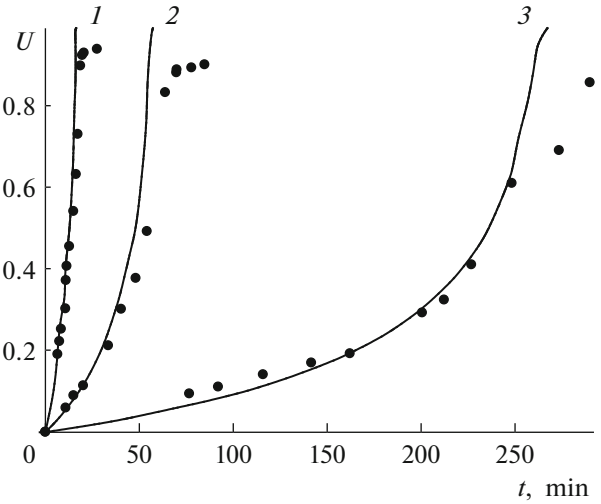

Fig. 1. Kinetic curves for the bulk radical polymerization of MMA initiated by azobisisobutyronitrile ($[I]_0$ = 15.5 mmol/L) at T = (*1*) 363, (*2*) 343, and (*3*) 323 K. The points represent experimental data [28], and the lines represent calculated data.

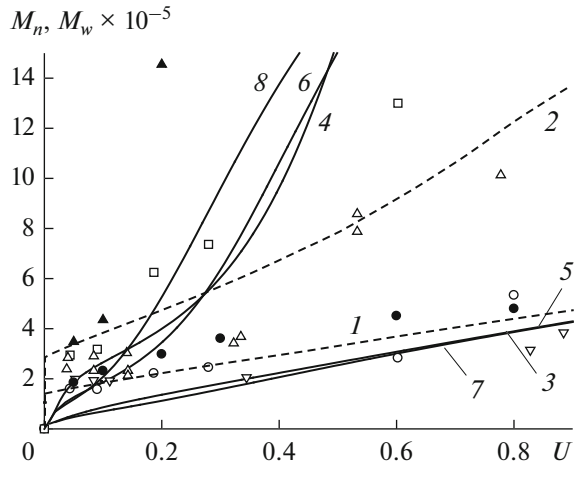

Fig. 2. (▽–*1*, ○–*3*, ○–*5*, ●–*7*) Number-average molecular weight and (△–*2*, □–*4*, □–*6*, ▲–*8*) weight-average molecular weight as a function of monomer conversion for PMMA obtained (*1*, *2*) by the bulk radical polymerization of MMA ($[M]_0$ = 9.4 mol/L) in the presence of BP ($[I]_0$ = 15.5 mmol/L) at T = 343 K and (*3*–*8*) by the bulk radical–coordination polymerization of MMA ($[M]_0$ = 9.4 mol/L) in the presence of the BP–ferrocene initiating system ($[I]_0$ = $[Mc]_0$ = 1 mmol/L) at T = (*3*–*6*) 333 K and (*7*, *8*) 343 K. Experimental data points: □, ○, ●, and ▲ [10, 11]; ▽ and △ [29]. Dashed lines: (*1*, *2*) data calculated for $[Mc]_0$ = 0. Solid lines: data calculated using the (*3*, *4*) first and (*5*–*8*) second mathematical kinetic models of the process.

$$\frac{d[M_{rad}]}{dt} = k_{prop1}[M]\mu_{10}, \quad \frac{d[M_{st}]}{dt} = k_{prop2}\mu_{50}.$$

In case the ferrocene concentration is zero, the mathematical models developed here describe the bulk radical polymerization of MMA with various initiators (depending on the temperature dependence of the constant k_{diss} used in the calculations).

The temperature dependences of the rate constants of the reactions involved in the bulk radical polymerization of MMA initiated by BP were taken from Refs. [21, 23, 24]:

$$k_{diss} = 1.18\times10^{14}e^{-15097/T}\ 1/s\ [21],$$

$$k_{rec0}/k_{disp0} = 3.956\times10^{-4}e^{2060/T}\ [23],$$

$$k_{rec0} + k_{disp0} = 9.8\times10^{7}e^{-353/T}\ L\,mol^{-1}\,s^{-1}\ [24],$$

where $k_{rec\,0}$ and $k_{disp\,0}$ are rate constants disregarding the gel effect.

The increase in the viscosity of the reaction mass in the course of the bulk radical polymerization mainly affects the rate constants of the reactions of two radicals. For this reason, using the model from Ref. [29], these constants were expressed as a function of MMA conversion (U) in the following way:

$$k_{rec} = k_{rec0}e^{-2(A_1U+A_2U^2+A_3U^3)}\ L\,mol^{-1}\,s^{-1},$$

$$k_{disp} = k_{disp0}e^{-2(A_1U+A_2U^2+A_3U^3)}\ L\,mol^{-1}\,s^{-1},$$

$$k_{adduct\,2} = k_{adduct\,20}e^{-2(A_1U+A_2U^2+A_3U^3)}\ L\,mol^{-1}\,s^{-1},$$

$$A_1 = a_{11} + a_{12}T,\ A_2 = a_{21} + a_{22}T,\ A_3 = a_{31} + a_{32}T,$$

where a_{ij} is a coefficient.

The values of a_{ij} ($A_1 = 31.52 - 0.074T$, $A_2 = 14.92 - 0.059T$, $A_3 = -38.66 + 0.132T$) and the temperature dependences of the rate constants $k_{prop\,1}$ ($k_{prop\,1} = 2.5\times10^{6}e^{-2820/T}$ L mol^{-1} s^{-1}) and k_{trans} ($k_{trans} = 2.79\times10^{5}e^{-5450/T}$ L mol^{-1} s^{-1}) were derived from the following experimental data: kinetic curves (MMA conversion U as a function of time t, see Fig. 1) [30] and the number- and weight-average molecular weights of PMMA as a function of monomer conversion (Fig. 2) [31] (processes: (1) bulk radical polymerization of MMA initiated by BP, (2) bulk radical polymerization of MMA initiated by azobisisobutyronitrile, for which it was accepted that $k_{diss} = 1.053\times10^{15}e^{-15440/T}$ 1/s [32]). This was done by minimizing the following functional by the Hooke–Jeeves method [33]:

$$\Phi = \sum_i\left(\frac{U_i^{calc} - U_i^{exp}}{U_i^{exp}}\right)^2 + \sum_i\left(\frac{M_{ni}^{calc} - M_{ni}^{exp}}{M_{ni}^{exp}}\right)^2 + \sum_i\left(\frac{M_{wi}^{calc} - M_{wi}^{exp}}{M_{wi}^{exp}}\right)^2,$$

where i is the ordinal number of the experimental data point, calc means a calculated value, and exp means an experimental value.

Next, we ascertained whether there are sets of remaining unknown constants at which the mathe-

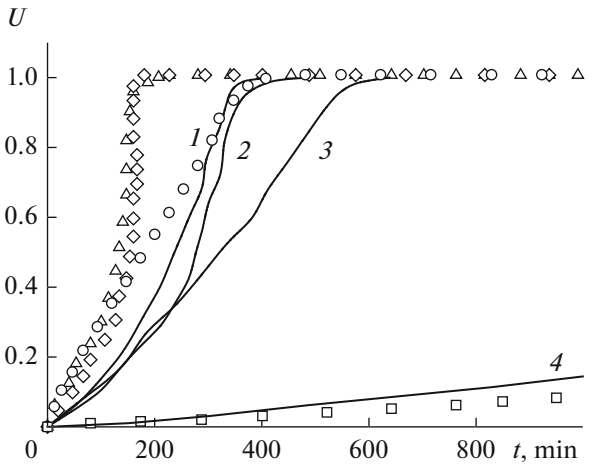

Fig. 3. Kinetic curves for the bulk radical–coordination polymerization of MMA in the presence of the BP–ferrocene initiating system (T = 333 K, $[M]_0$ = 9.4 mol/L, $[I]_0$ = 1 mmol/L) at various initial ferrocene concentrations: $[Mc]_0$ = (△–*1*) 0.2, (◇–*2*) 0.5, (○–*3*) 1, and (□–*4*) 8 mmol/L. The points represent experimental data [9–11], and the lines represent the data calculated using the first mathematical kinetic model of the process.

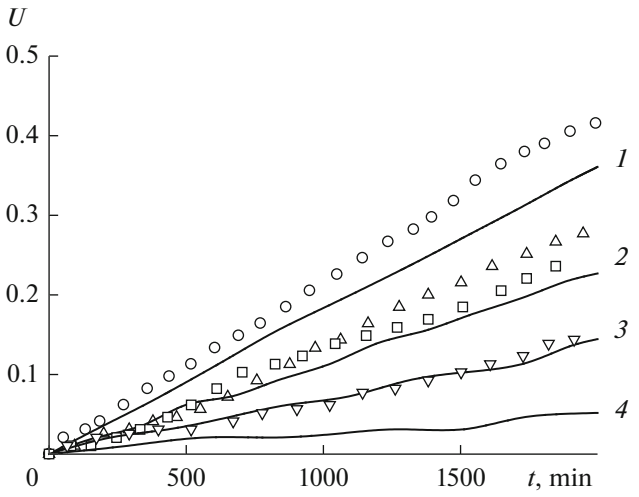

Fig. 4. Kinetic curves for the bulk postpolymerization of MMA initiated by the PMMA macroinitiator that was synthesized by the bulk radical–coordination polymerization of MMA in the presence of the BP–ferrocene initiating system (PMMA macroinitiator synthesis conditions: T = 333 K, $[M]_0$ = 9.4 mol/L, $[I]_0$ = $[Mc]_0$ = 1 mmol/L). The PMMA macroinitiator was sampled at MMA conversions of (○–*1*) 0.05, (△–*2*) 0.1, (□–*3*) 0.2, and (▽–*4*) 0.6. The points represent experimental data [12], and the lines represent the data calculated using the fits mathematical kinetic model of the process.

matical kinetic models developed for the radical–coordination polymerization of MMA will fit experimental data within the experimental error (25% for MMA conversion [22] and 35% for the M_n and M_w of PMMA [34]).

The following data were considered (all of them refer to one temperature of 333 K; otherwise, it would be necessary to determine not the values of rate constants but their temperature dependences and this would increase the number of unknowns but would not facilitate the construction of the kinetic scheme):

kinetic curves for the bulk radical–coordination polymerization of MMA initiated by the BP–ferrocene system ($[I]_0$ = 1 mmol/L, $[M]_0$ = 9.4 mol/L, and $[Mc]_0$ = 0.2, 0.5, 1, and 8 mmol/L) [9–11];

conversion-dependent M_n and M_w data for PMMA synthesized by the bulk radical–coordination polymerization of MMA initiated by the BP–ferrocene system ($[I]_0$ = 1 mmol/L, $[M]_0$ = 9.4 mol/L, and $[Mc]_0$ = 1 mmol/L) [10, 11];

stereoregularity (γ) data for PMMA synthesized by the bulk radical–coordination polymerization of MMA initiated by the BP–ferrocene system ($[I]_0$ = 1 mmol/L, $[M]_0$ = 9.4 mol/L, and $[Mc]_0$ = 0.2 and 1 mmol/L) [8];

kinetic curves for the bulk postpolymerization of MMA in the presence of a macroinitiator, whose role was played by PMMA samples that were obtained by the bulk radical–coordination polymerization of MMA initiated by the BP–ferrocene system and were isolated at an MMA conversion of 0.05, 0.1, 0.2, or 0.6 ($[I]_0$ = 0 mmol/L; $[M]_0$ = 9.4 mol/L; initial weight fraction of the PMMA macroinitiator, 3%) [12].

Based on available experimental data, we sought the rate constants for the reactions of both kinetic schemes by minimizing the functional

$$\Phi = \sum_i \left(\frac{U_i^{calc} - U_i^{exp}}{U_i^{exp}} \right)^2 + \sum_i \left(\frac{M_{ni}^{calc} - M_{ni}^{exp}}{M_{ni}^{exp}} \right)^2 + \sum_i \left(\frac{M_{wi}^{calc} - M_{wi}^{exp}}{M_{wi}^{exp}} \right)^2 + \sum_i \left(\frac{\gamma_i^{calc} - \gamma_i^{exp}}{\gamma_i^{exp}} \right)^2$$

by the Hooke–Jeeves method [33].

Minimization of the functional for the first mathematical kinetic model of the process yielded the following values of the rate constants: k_{compl} = 5.27 L mol^{-1} s^{-1}, $k_{in\,1} = 6.3 \times 10^{-4}$ L mol^{-1} s^{-1}, $k_{in\,2} = 1.53 \times 10^{-5}$ L mol^{-1} s^{-1}, $k_{adduct\,1} = 4.6 \times 10^4$ L mol^{-1} s^{-1}, $k_{adduct\,20} = 3.75 \times 10^4$ L mol^{-1} s^{-1}, $k_{add\,1} = 1.27 \times 10^3$ L mol^{-1} s^{-1}, k_{coord} = 0.118 L mol^{-1} s^{-1}, and $k_{prop\,2}$ = 0.158 1/s.

The kinetic curves and M_n, M_w, and γ data calculated for PMMA according to the first kinetic model of the process are presented in Figs. 2–4.

The mean relative errors in the calculations according to the first kinetic model are the following: for U (Fig. 1), 56%; for M_n (Fig. 3), 37%; for M_w (Fig. 3), 39%; for U (Fig. 4), 37%; for γ, 2%. At $[Mc]_0$ = 0.2 mmol/L, the experimental value of the stereoregularity of PMMA is γ = 59.0% [8] and the calculated

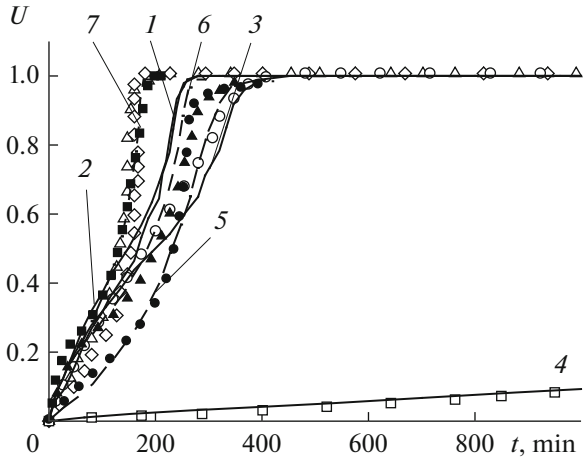

Fig. 5. Kinetic curves for the bulk radical–coordination polymerization of MMA in the presence of the BP–ferrocene initiating system ($[M]_0$ = 9.4 mol/L, $[I]_0$ = 1 mmol/L) at initial ferrocene concentrations of $[Mc]_0$ = (△–*1*) 0.2, (◇–*2*) 0.5, (◇–*3*, ●–*5*, ▲–*6*, ■–*7*) 1, and (□–*4*) 8 mmol/L and temperatures of *T* = (●–*5*) 313, (△–*1*, ◇–*2*, ○–*3*, □–*4*) 333, (▲–*6*) 343, and (■–*7*) 353 K. The points represent experimental data [9–11], and the lines represent the data calculated using the second mathematical kinetic model of the process.

stereoregularity is γ = 57.3%; at $[Mc]_0$ = 1 mmol/L, the experimental stereoregularity is γ = 65.0% [8] and the calculated stereoregularity is γ = 64.5%.

Prior to minimizing the functional for the second mathematical model of polymerization kinetics, we reduced the number of unknown rate constants in the second kinetic scheme. For this purpose, we initially analyzed the experimental kinetic curves shown in Fig. 4. Since, in the PMMA-initiated bulk postpolymerization of MMA, the monomer polymerizes on the coordination active site Ad_3, this process is described by the following system of equations:

$$\frac{d[M]}{dt} = -k_{coord}\mu_{40}[M], \quad (1)$$

$$\frac{d\mu_{40}}{dt} = -k_{coord}[M]\mu_{40} + k_{prop2}\mu_{50}, \quad (2)$$

$$\frac{d\mu_{50}}{dt} = k_{coord}[M]\mu_{40} - k_{prop2}\mu_{50}. \quad (3)$$

The sum of Eqs. (2) and (3) is zero, so the total concentration of Ad_2 and Ad_3 constant:

$$\mu_{40}\big|_{t=0} + \mu_{50}\big|_{t=0} = \mu_{40} + \mu_{50}. \quad (4)$$

According to the quasi-steady-state approximation,

$$0 = -k_{coord}[M]\mu_{40} + k_{prop2}\mu_{50}. \quad (5)$$

By simultaneously solving Eqs. (4) and (5), we obtain

$$\mu_{40} = \frac{k_{prop2}}{k_{prop2} + k_{coord}[M]}\left(\mu_{40}\big|_{t=0} + \mu_{50}\big|_{t=0}\right).$$

Substituting this formula into Eq. (1), we obtain

$$\frac{d[M]}{dt} = -k_{coord}[M] \times \frac{k_{prop2}}{k_{prop2} + k_{coord}[M]}\left(\mu_{40}\big|_{t=0} + \mu_{50}\big|_{t=0}\right).$$

Because the kinetic curves for the bulk postpolymerization of MMA initiated by PMMA are rectilinear, we have

$$\frac{d[M]}{dt} = \text{const},$$

$$k_{coord}[M]\frac{k_{prop2}}{k_{prop2} + k_{coord}[M]} \times \left(\mu_{40}\big|_{t=0} + \mu_{50}\big|_{t=0}\right) = \text{const}.$$

This condition is satisfied at $k_{prop\,2} \ll k_{coord}[M]$. In case the reverse reactions take place, releasing radicals from the Ad_2 and Ad_3 structures, the resulting radicals undergo recombination and disproportionation. As a consequence, not all of the dissociated Ad_2 and Ad_3 adducts are recovered and their concentrations decrease, so

$$k_{coord}[M]\frac{k_{prop2}}{k_{prop2} + k_{coord}[M]} \times \left(\mu_{40}\big|_{t=0} + \mu_{50}\big|_{t=0}\right) \neq \text{const}$$

and the kinetic curves for the bulk postpolymerization of MMA initiated by PMMA cannot be rectilinear. The constants $k_{adduct\,3}$, $k_{adduct\,4}$, $k_{diss\,3}$, $k_{diss\,4}$, and $k_{add\,2}$ were finally taken to be zero, because the corresponding reactions do not occur.

Minimization of the functional for the second mathematical model of polymerization kinetics yielded the following values of rate constants: k_{compl} = 11 L mol^{-1} s^{-1}, $k_{diss\,1} = 1.36 \times 10^{-3}$ 1/s, $k_{adduct\,1}$ = 38800 L mol^{-1} s^{-1}, $k_{adduct\,20}$ = 11 300 L mol^{-1} s^{-1}, $k_{diss\,2} = 3.77 \times 10^{-2}$ s^{-1}, $k_{add\,1} = 7 \times 10^{-4}$ L mol^{-1} s^{-1}, $k_{coord} = 2.79 \times 10^{-1}$ L mol^{-1} s^{-1}, and $k_{prop\,2} = 2.37 \times$ 1/s.

The kinetic curves and M_n, M_w, and γ data calculated for PMMA according to the second mathematical model of polymerization kinetics are plotted in Figs. 2, 5, and 6.

The mean relative errors in the calculations according to the second kinetic model are the following: for *U* (Fig. 1), 22%; for M_n (Fig. 3), 17%; for M_w (Fig. 3), 32%; for *U* (Fig. 4), 15%; for γ, 2%. At $[Mc]_0$ = 0.2 mmol/L, the experimental value of the stereoregularity of PMMA is γ = 59.0% [8] and the calculated value is γ = 57.2%; at $[Mc]_0$ = 1 mmol/L, the experimental stereoregularity is γ = 65.0% [8] and the calculated stereoregularity is γ = 65.6%.

The computational errors for the first model of polymerization kinetics are much larger than the

errors for the second model. The errors for the first model are larger than the corresponding experimental errors (25% for MMA conversion [22] and 35% for the M_n and M_w of PMMA [34]). Therefore, the bulk radical–coordination polymerization of MMA initiated by the BP–ferrocene system most likely takes place according to the scheme that includes the reactions typical of classical radical polymerization and also reactions specific to controlled radical polymerization proceeding via the OMRP mechanism and coordination active site formation and chain propagation reactions in the coordination sphere of the metal.

Next, we demonstrated the adequacy of the mathematical model of the kinetics of the process. For this purpose, we determined the ratio of the residual variance S_{res} (measure of the deviation of calculated data from experimental data) to the reproducibility variance S_{repr} (which characterizes the experimental error) for all time dependences of MMA conversion at 333 K,

$$\frac{S_{res}}{S_{repr}} = \frac{0.0602}{0.0625} = 0.9632,$$

and for the time dependences of the M_n and M_w of PMMA at 333 K,

$$\frac{S_{res}}{S_{repr}} = \frac{0.063}{0.123} = 0.512.$$

The variances were calculated from relative deviation values; S_{repr} was calculated as the square of the standard deviation—0.25 for U and 0.35 for M_n and M_w.

The variance ratios thus determined do not exceed the Fisher criterion values for the given number of experimental data points and a significance level of 0.05: 1.35 for U and 1.92 for M_n and M_w. For this reason, the second mathematical model of polymerization kinetics was accepted to be adequate.

In order to extend the second mathematical model to calculation of U, M_n, M_w, PD, and γ at temperatures other than 333 K, the rate constants of the reactions were set as their temperature dependences according to the Arrhenius equation

$$k(T) = Be^{-E/(RT)},$$

where B is the preexponential factor (in 1/s units for unimolecular reactions and in L mol^{-1} s^{-1} units for bimolecular ones), E is the activation energy (J/mol), $R = 8.31$ J mol^{-1} K^{-1} is the gas constant, and T is temperature (K).

The unknowns in the Arrhenius equation for each rate constant are E and B. However, since the values of the rate constants at 333 K are known, E and B for each rate constant are related as $B = ke^{E/(333R)}$. Accordingly, determination of the temperature dependences of the rate constants actually reduced to finding E for each rate constant.

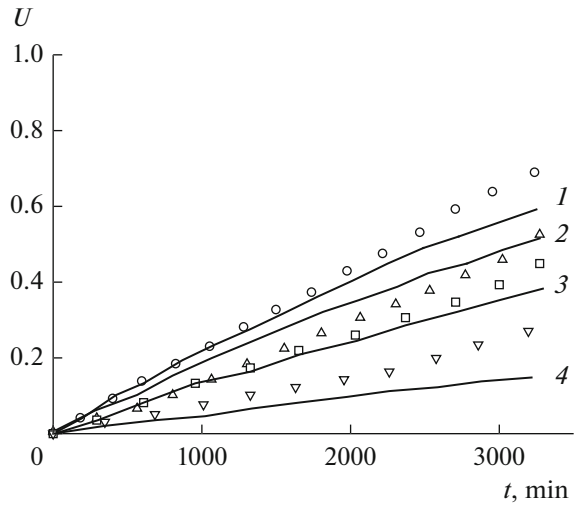

Fig. 6. Kinetic curves for the bulk postpolymerization of MMA initiated by the PMMA macroinitiator that was synthesized by the bulk radical–coordination polymerization of MMA in the presence of the BP–ferrocene initiating system (MMA macroinitiator synthesis conditions: T = 333 K, $[M]_0 = 9.4$ mol/L, $[I]_0 = [Mc]_0 = 1$ mmol/L). The PMMA macroinitiator was sampled at MMA conversions of (○–*1*) 0.05, (△–*2*) 0.1, (□–*3*) 0.2, and (▽–*4*) 0.6. The points represent experimental data [12], and the lines represent the data calculated using the second mathematical kinetic model of the process.

The E values were determined in the same way as the rate constants at 333 K by solving the inverse kinetic problem. The following eight quantities were sought: E_{compl}, $E_{diss\ 1}$, $E_{adduct\ 1}$, $E_{adduct\ 2}$, $E_{diss\ 2}$, $E_{add\ 1}$, E_{coord}, and $E_{prop\ 2}$ (the subscripts correspond to reactions in Table 1).

The following experimental data were used to determine E:

kinetic curves for the bulk radical–coordination polymerization of MMA initiated by the BP–ferrocene system ($[I]_0 = [Mc]_0 = 1$ mmol/L) at T = 313, 333, 343, 353 K [9];

number-average molecular weight M_n and weight-average molecular weight M_w as a function of monomer conversion for PMMA obtained by the bulk radical–coordination polymerization of MMA initiated by the BP–ferrocene system ($[I]_0 = [Mc]_0 = 1$ mmol/L, $[M]_0 = 9.4$ mol/L) at 333 K [11] and 343 K.

The E_{compl}, $E_{diss\ 1}$, $E_{adduct\ 1}$, $E_{adduct\ 2}$, $E_{diss\ 2}$, $E_{add\ 1}$, E_{coord}, and $E_{prop\ 2}$ values were determined by minimizing the functional

$$\Phi = \sum_i \left(\frac{U_i^{calc} - U_i^{exp}}{U_i^{exp}} \right)^2 + \sum_i \left(\frac{M_{ni}^{calc} - M_{ni}^{exp}}{M_{ni}^{exp}} \right)^2 + \sum_i \left(\frac{M_{wi}^{calc} - M_{wi}^{exp}}{M_{wi}^{exp}} \right)^2$$

Table 2. Kinetic scheme suggested for the bulk radical–coordination polymerization of MMA in the presence of the BP–ferrocene initiating system and the temperature dependences of the rate constants

Reaction designation*	k at 333 K**	$k(T)$**
$I \xrightarrow{k_{diss}} 2R(0)$	$K_{diss} = 2.72 \times 10^{-6}$	$k_{diss} = 1.18\times10^{14}e^{-15097/T}$ [3]
$R(0) + M \xrightarrow{k_{prop1}} R(1)$	$k_{propl} = 520^{+26}_{-42}$	$k_{prop1} = 2.5\times10^{6}e^{-2810/T}$
$R(n) + M \xrightarrow{k_{prop1}} R(n+1)$	$k_{propl} = 520^{+26}_{-42}$	$k_{prop1} = 2.5\times10^{6}e^{-2810/T}$
$R(n) + M \xrightarrow{k_{trans}} R(1) + P(n)$	$k_{trans} = 2.17^{+4.12}_{-0.41}\times10^{-2}$	$k_{trans} = 2.79\times10^{5}e^{-5450/T}$
$R(n) + R(z) \xrightarrow{k_{rec}} P(n+z)$ $R(n) + R(z) \xrightarrow{k_{disp}} P(n) + P(z)$	$k_{rec} = 2.85\times10^{7}e^{-2\sum_{i=1}^{3}A_iU^i}$, $k_{disp} = 5.47\times10^{6}e^{-2\sum_{i=1}^{3}A_iU^i}$, $A_i = a_{i1} + a_{i2}333$, $a_{11} = 31.5^{+0.3}_{-0.3}$, $a_{12} = -0.074^{+0.001}_{-0.001}$ 1/K, $a_{21} = 14.92^{+0.75}_{-0.9}$, $a_{22} = -0.059^{+0.002}_{-0.002}$ 1/K, $a_{31} = -38.66^{+1.55}_{-1.55}$, $a_{32} = 0.132^{+0.005}_{-0.004}$ 1/K	$k_{rec} = \frac{3.877\times10^{4}e^{1707/T}}{3.956\times10^{-4}e^{2060/T}+1}e^{-2\sum_{i=1}^{3}A_iU^i}$, $k_{disp} = \frac{9.8\times10^{7}e^{-353/T}}{3.956\times10^{-4}e^{2060/T}+1}e^{-2\sum_{i=1}^{3}A_iU^i}$, $A_i = a_{i1} + a_{i2}T$, $a_{11} = 31.5^{+0.3}_{-0.3}$, $a_{12} = -0.074^{+0.001}_{-0.001}$ 1/K, $a_{21} = 14.92^{+0.75}_{-0.9}$, $a_{22} = -0.059^{+0.002}_{-0.002}$ 1/K, $a_{31} = -38.66^{+1.55}_{-1.55}$, $a_{32} = 0.132^{+0.005}_{-0.004}$ 1/K
$I + Mc \xrightarrow{k_{compl}} Ad_1(0) + R(0)$	$k_{compl} = 11^{+5.94}_{-4.84}$	$k_{compl} = 1.18^{+0.4}_{-0.45}\times10^{6}e^{-\frac{32040^{+1090}_{-900}}{RT}}$
$Ad_1(0) \xrightarrow{k_{diss1}} Mc + R(0)$	$k_{propl} = 1.36^{+0.6}_{-0.49}\times10^{-3}$	$k_{prop1} = 4.27^{+1.11}_{-1.02}\times10^{16}e^{-\frac{124230^{+750}_{-500}}{RT}}$
$Mc + R(n) \xrightarrow{k_{adduct1}} Ad_1(n)$	$k_{adduct1} = 3.88^{+1.94}_{-0.39}\times10^{4}$	$k_{adduct\,1} = 1.97^{+1.02}_{-0.51}\times10^{10}e^{-\frac{36360^{+800}_{-1090}}{RT}}$
$R(z) + Ad_1(n) \underset{k_{diss2}}{\overset{k_{adduct2}}{\rightleftarrows}} Ad(n,z)$	$k_{adduct2} = 1.13^{+0.16}_{-0.36}\times10^{4}$, $k_{diss2} = 3.77^{+2.11}_{-0.53}\times10^{-2}$	$k_{adduct\,2} = 7.80^{+3.43}_{-1.72}\times10^{8}e^{-\frac{30830^{+740}_{-1050}}{RT}}e^{-2\sum_{i=1}^{3}A_iU^i}$, $k_{diss\,2} = 1.01^{+0.34}_{-0.34}\times10^{19}e^{-\frac{130160^{+1040}_{-780}}{RT}}$
$Ad(n,z) + M \xrightarrow{k_{add1}} Ad_2(z) + P(n)$	$k_{add1} = 7.00^{+1.12}_{-2.52}\times10^{-4}$	$k_{add1} = 1.17^{+0.59}_{-0.3}\times10^{10}e^{-\frac{84250^{+840}_{-1180}}{RT}}$
$Ad_2(z) + M \xrightarrow{k_{coord}} Ad_3(z)$***	$k_{coord} = 2.79^{+0.95}_{-1.17}\times10^{-1}$	$k_{coord} = 6.23^{+1.37}_{-1.25}\times10^{4}e^{-\frac{34080^{+680}_{-550}}{RT}}$
$Ad_3(z) \xrightarrow{k_{prop2}} Ad_2(z+1)$***	$k_{prop2} = 2.37^{+0.78}_{-1.04}$	$k_{prop2} = 5.29^{+1.8}_{-1.27}\times10^{5}e^{-\frac{34080^{+820}_{-750}}{RT}}$

* $n = 1, \ldots$ and $z = 1, \ldots$ are the numbers of MMA units in polymer chains.

** Units of measurement: rate constants of unimolecular reactions, 1/s; rate constants of bimolecular reactions, L mol^{-1} s^{-1}; E in $k(T)$, J/mol; gas constant, $R = 8.31$ J mol^{-1} K^{-1}; T, K.

*** Reactions from the kinetic scheme of the bulk postpolymerization of MMA in the presence of the PMMA macroinitiator.

by the Hooke–Jeeves method [33]. Here, i is the ordinal number of an experimental data point, calc means the calculated value, and exp means the experimental value.

The calculated temperature dependences of the rate constants are presented in Table 2.

The kinetic curves for the process and M_n and M_w data for PMMA calculated according to the mathematical kinetic model with the B and E values determined are presented in Figs. 2, 5, and 6.

The mean relative errors in the calculation of the kinetics of the process according to the mathematical model are the following: for U (Fig. 5, curves *3*, *5*–*7*), 8%; for M_n (Fig. 2), 17%; for M_w, 30% (Fig. 2). Since these errors do not exceed the experimental errors (25% for MMA conversion and 35% for the M_n and M_w of PPMA), the found set of E_{compl}, $E_{diss\ 1}$, $E_{adduct\ 1}$, $E_{adduct\ 2}$, $E_{diss\ 2}$, $E_{add\ 1}$, E_{coord}, and $E_{prop\ 2}$ is a solution of the inverse kinetic problem. In order to pass from this partial solution to the general solution, we determined, for each E value, the uncertainty interval that provides a fit the experimental data without the experimental error being exceeded. In the calculation of the uncertainty interval for a particular E or B, the other E and B values were fixed. The results of this calculation are presented in Table 2.

CONCLUSIONS

Thus, we have constructed the kinetic scheme of the bulk radical–coordination polymerization of MMA initiated by the BP–ferrocene system and have determined the temperature dependences of the rate constants of the reactions appearing in this scheme. The mathematical model developed on the basis of this kinetic scheme for the kinetics of the process provides means to calculate not only the kinetics of the main process but also the kinetics of the postprocess—MMA polymerization occurring on "living" coordination active sites of PMMA, which results from the main process and act as a macroinitiator in the postprocess (i.e., the reactions inherent in the kinetic scheme of the post process are included in the kinetic scheme of the main process, and this means that the mathematical model of the kinetics of the main process at zero values of the rate constants of the other reactions of the kinetic scheme will describe the kinetics of the postprocess). In addition, the mathematical kinetic model makes it possible to calculate the molecular weight characteristics and stereoregularity of PMMA (which forms both in the main process and in the postprocess).

The mathematical kinetic model developed in this study enables can be used to perform a multifactor numerical experiment in order to reveal the effects of some factors (reactant concentrations and temperature) on the rates of the main process and postprocess and on the molecular weight characteristics and stereoregularity of PMMA forming in these two processes.

ACKNOWLEDGMENTS

This study was supported by the Russian Foundation for Basic Research, project no. 16-33-50186 mol_nr.

REFERENCES

1. Korolev, G.V. and Marchenko, A.P., *Russ. Chem. Rev.,* 2000, vol. 69, no. 5, p. 409.
2. Grishin, I.D., Chizhevsky, I.T., and Grishin, D.F., *Kinet. Catal.,* 2009, vol. 50, no. 4, p. 550.
3. Chernikova, E.V., Terpugova, P.S., Garina, E.S., and Golubev, V.B., *Polym. Sci., Ser. A,* 2007, vol. 49, no. 2, p. 108.
4. Ulitin, N.V., Shirokikh, E.B., Nasyrov, I.I., Kalinina, D.Sh., Sidel'nikova, V.A., Samarin, E.V., and Deberdeev, R.Ya., *Kinet. Catal.,* 2014, vol. 55, no. 2, p. 154.
5. *Controlled/"Living" Radical Polymerization: Progress in ATRP,* Matyjaszewski, K., Ed., Washington, DC: Am. Chem. Soc., 2009.
6. *Controlled/"Living" Radical Polymerization: Progress in RAFT, DT, NMP and OMRP,* Matyjaszewski, K., Ed., Washington, DC: Am. Chem. Soc., 2009.
7. *Handbook of RAFT Polymerization,* Barner-Kowollik, C., Ed., Weinheim, Germany: Wiley–VCH, 2008.
8. Puzin, Yu.I., Yumagulova, R.Kh., Kraikin, V.A., Ionova, I.A., and Prochukhan, Yu.A., *Polym. Sci., Ser. B,* 2000, vol. 42, nos. 3–4, p. 90.
9. Sigaeva, N.N., Frizen, A.K., Nasibullin, I.I., Ermolaev, N.L., and Kolesov, S.V., *Kinet. Catal.,* 2012, vol. 53, no. 4, p. 470.
10. Sigaeva, N.N., Yumagulova, R.Kh., Frizen, A.K., and Kolesov, S.V., *Polym. Sci., Ser. B,* 2009, vol 51, nos. 7–8, p. 226.
11. Sigaeva, N.N., Yumagulova, R.Kh., Nasretdinova, R.N., Frizen, A.K., and Kolesov, S.V., *Kinet. Catal.,* 2009, vol. 50, no. 2, p. 168.
12. Kolesov, S.V., Nasibullin, I.I., Frizen, A.K., Sigaeva, N.N., and Galkin, E.G., *Polym. Sci., Ser. B,* 2015, vol. 57, no. 2, p. 71.
13. Murinov, Y.I., Grabovskiy, S.A., Islamova, R.M., Kuramshina, A.R., and Kabal'nova, N.N., *Mendeleev Commun.,* 2013, vol. 23, p. 53.
14. Grognes, E.L., Claverie, J., and Poli, R., *J. Am. Chem. Soc.,* 2001, vol. 123, p. 9513.
15. Ochedzan-Siodlak, W. and Nowakowska, M., *Eur. Polym. J.,* 2005, vol. 41, p. 941.
16. Wilson, P.A., Hannant, M.H., Wright, J.A., Cannon, R.D., and Bochmann, M., *Macromol. Symp.,* 2006, vol. 236, p. 100.
17. Resconi, L., Cavallo, L., Fait, A., and Piemontesi, F., *Chem. Rev.,* 2000, vol. 100, no. 4, p. 1253.
18. Filho, A.P.O., Souza, J.L., and Schuchardt, U., *Stud. Surf. Sci. Catal.,* 2000, vol. 130, p. 329.

19. Sigaeva, N.N., Frizen, A.K., Nasibullin, I.I., Ermolaev, N.L., and Kolesov, S.V., *Polym. Sci., Ser. B,* 2012, vol. 54, p. 197.
20. Frizen, A.K., Khursan, S.L., Kolesov, S.V., and Monakov, Yu.B., *Russ. J. Phys. Chem. B,* 2011, vol. 5, no. 1, p. 131.
21. Bagdasar'yan Kh.S., *Theory of Free-Radical Polymerization*, Jerusalem: Israel Program for Scientific Translations, 1968.
22. Brandrup, J., Immergut, E.H., and Grulke, E.A., *Polymer Handbook,* New York: Wiley, 1999.
23. Baillagou, P.E. and Soong, D.S., *Chem. Eng. Sci.,* 1985, vol. 40, no. 1, p. 87.
24. Mahabadi, H.K. and O'Driscoll, K.F., *J. Macromol. Sci., Part A,* 1977, vol. 11, no. 5, p. 967.
25. Bevington, J.C., Melville, H.W., and Taylor, R.P., *J. Polym. Sci.,* 1954, vol. 14, no. 2, p. 463.
26. Ulitin, N.V., Tereshchenco, K.A., Shiyan, D.A., and Zaikov, G.E., *Rubber Chem. Technol.,* 2015, vol. 88, no. 4, p. 574.
27. Ulitin, N.V. and Tereshchenko, K.A., *Kinet. Catal.*, 2016, vol. 57, no. 2, p. 170.
28. Ulitin, N.V. and Tereshchenko, K.A., *Kinet. Catal.,* 2016, vol. 57, no. 2, p. 177.
29. Hui, A.W. and Hamielec, A.E., *J. Appl. Polym. Sci.,* 1972, vol. 16, p. 749.
30. Balke, S., Garcia-Rubio, L., and Patel, R., *Polym. Eng. Sci.,* 1982, vol. 22, no. 12, p. 777.
31. Balke, S.T. and Hamielec, A.E., *J. Appl. Polym. Sci.,* 1973, vol. 17, p. 905.
32. Tobolsky, A.V. and Baysal, B., *Polym. Sci.,* 1953, vol. 11, no. 5, p. 471.
33. Dolan, E.D., Lewis, R.M., and Torczon, V.J., *SIAM J. Optim.,* 2003, vol. 14, no. 2, p. 567.
34. *Ultra-High Performance Liquid Chromatography and Its Applications,* Quanyun Alan Xu, Ed., New Jersey: Wiley, 2013.

Translated by D. Zvukov